RADIOISOTOPES, **64**, 169-176 (2015)

Article

Application of ^{42}K to Arabidopsis Tissues Using Real-Time Radioisotope Imaging System (RRIS)

Toshinori ARAMAKI, Ryohei SUGITA, Atsushi HIROSE, Natsuko I. KOBAYASHI, Keitaro TANOI† and Tomoko M. NAKANISHI

Graduate School of Agricultural and Life Sciences, The University of Tokyo
1-1-1 Yayoi, Bunkyo-ku, Tokyo 113-8657, Japan
†uktanoi@mail.ecc.u-tokyo.ac.jp

Received September 16, 2014
Accepted January 13, 2015

We performed an imaging analysis of ^{42}K in Arabidopsis using real-time radioisotope imaging system (RRIS). First, we purified ^{42}K from an ^{42}Ar–^{42}K generator. And then, we characterized RRIS performance by quantitatively determining ^{42}K using standard series. As a result, the dynamic range for ^{42}K was determined to be at least three orders of magnitude. Next, we evaluated the level of self-absorption in Arabidopsis organs by comparing the signal intensity detected using RRIS and the actual radioactivity detected by a gamma-counting method. There was no significant difference in detection efficiency between the thick bolt (stem) tissue and the thin leaf tissue. The reason for scarce self-absorption could be related to the relatively strong β ray emissions that have a maximum energy of 3 525.4 keV.

Key Words : potassium-42, distribution, real-time radioisotope imaging system (RRIS), plant nutrition, long-distance transport

1. Introduction

Potassium (K) is one of the major essential elements in plants and its physiological role and the role of transporters mediating the transmembrane K transport within plant tissues have been intensively studied[1)-3)]. Despite this, the behavior of long-distance K transport in a plant, the organ to which K is transported after it has been absorbed by the root, and the factors affecting K transport have not yet been clarified. Knowledge of long-distance K transport has been obtained from data concerning distributions and functions of K transporters, or changes in tissue K concentrations[4)-6)]. The development of a new technique that uses a K isotope in combination with a sequential detection method, or live-imaging method, would be a highly effective tool for understanding K behavior in a living plant.

Because radioisotopes of K are not commercially available, Rubidium-86 (^{86}Rb), which is thought to behave similarly to K in plants, has been substituted as a tracer for K[2),7),8)]. However, there is no evidence that Rb undertakes the physiological role of K or whether it completely traces the behavior of K[9)]. For example, when ^{86}Rb was used as a K^+ label in an uptake study using barley, values were reported to be underestimated[10)]. To accurately observe K movement, it is best to employ K isotopes as tracers.

^{40}K is a well-known natural radioactive isotope of K, but there are few reports of it being used as a tracer because it is difficult to produce and obtain pure radioisotopes. In addition, ^{38}K has been employed as a tracer in rabbits[11] and rice[12] and it was produced using a cyclotron[13]. However, the half-life of ^{38}K, 7.6 m, is very short for analyzing movement that takes more than 1 h, and consequently this short-life nuclide is not suitable for plant analysis. Another radioactive isotope, ^{42}K (main β-ray: mean energy 1 566.0 keV, maximum energy 3 525.4 keV, 81.90%, main γ-ray: 1 524.6 keV, 18.08%), has the potential to be used as a tracer, and the kinetics of K in a plant root using ^{42}K produced in a nuclear reactor have been reported[14),15].

However, using ^{42}K in an imaging experiment has two problems regarding the feature of ^{42}K. Firstly, ^{42}K is a β^- and γ-ray emitter, not a β^+ emitter. At present, most radionuclide imaging apparatus are based on positron emission tomography (PET) and use positron-emitting nuclides generated in a type of accelerator[16),17]. Meanwhile, the real-time radioisotope imaging system (RRIS), which we developed in Japan, has the potential to sequentially detect radiation from ^{42}K because RRIS is highly sensitive to β-rays as well as X-rays[18),19]. The second problem with ^{42}K is that it has a relatively short half-life (12.36 h). This means that ^{42}K is neither commercially available at present nor transportable over a long distance. Therefore, we used the ^{42}K milking system and set up the ^{42}Ar–^{42}K generator near the RRIS experiment area to obtain ^{42}K just before experiments.

In this report, we quantitatively evaluated the imaging of ^{42}K using RRIS and applied it to the dynamic analysis of K transport in intact plants. In addition, we considered the effect of self-absorption, which is the shielding effect by the plant tissue itself to radioactivity. In cases where β-ray-emitting nuclides were used as tracers, there was concern that self-absorption of weak β-rays in plant samples affects quantitative efficiency[19]. Although the energy of β-rays from ^{42}K are relatively strong (maximum energy = 3 525.4 keV), there is a little possibility of self-absorption. Thus, to assess the practical usefulness of ^{42}K for imaging in plant physiology research, we evaluated the level of self-absorption using *Arabidopsis* tissues and compared the signal intensity detected by RRIS with the radioactivity detected by the γ-ray counting method.

2. Materials and methods

2·1 Plant materials

Arabidopsis thaliana plants were grown on MGRL culture solution for plants[20] for 4 – 5 weeks in a growth chamber at 22℃ with 16-h light period and 8-h dark period.

2·2 Preparation of the ^{42}K solution

^{42}K was obtained from the ^{42}Ar–^{42}K generator using the method [21] with minor modifications. In this generator, ^{42}Ar, whose half-life is approximately 33 years, decays to continuously produce ^{42}K. ^{42}Ar was produced by the ^{40}Ar(t, p)^{42}Ar reaction in a cyclotron[22]. A steel cathode was inserted into a generator and approximately 60 V was applied to accumulate ^{42}K with a positive charge (Fig. 1). This cathode was then washed for 10 m to obtain approximately 5 000 Bq of ^{42}K solution in a 0.5 mM KCl solution or in the MGRL culture solution. The radioactivity of the extracted solution was measured using a liquid scintillation counter (LSC 6100, ALOKA).

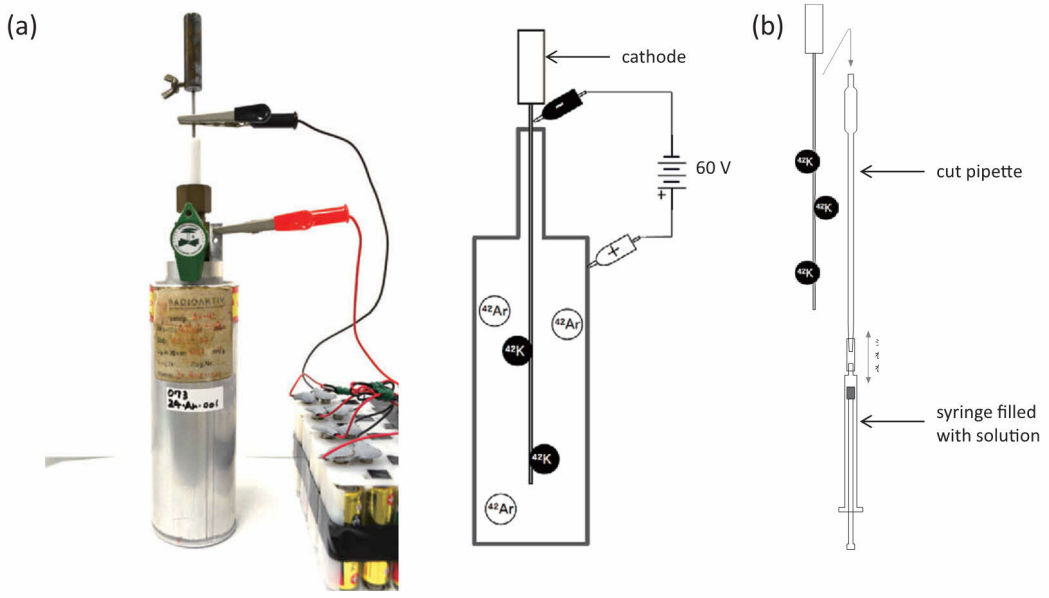

Fig. 1 (a) Picture and schematic drawing of the ^{42}Ar–^{42}K generator. A charge of 60 V was applied to the cathode to attract ionized ^{42}K. (b) The method for extracting ^{42}K from the cathode. A syringe filled with extracting solution was attached to the tip of a cut pipette and the cathode was inserted into the opposite end of the pipette. The solution was pushed into the pipette from the syringe to immerse and wash the cathode. The ^{42}K solution was then collected in the syringe and the cathode was replaced into the generator.

2・3 Verification of determination range

Dilution series of 2 μL (approximately 1 – 1 000 Bq/mm^2) were spotted on a polyethylene terephthalate sheet and covered with polyethylene film. Radioactivities of the spots were measured using RRIS. The detailed structure of RRIS apparatus and the measuring method are described in Sugita *et al*. (2014)[19]. The image data from RRIS were processed using AQUACOSMOS software (Hamamatsu Photonics).

2・4 Verification of self-absorption by plant samples

Arabidopsis plants were transferred to MGRL culture solution containing ^{42}K (2 – 2.5 mL, approximately 5 000 Bq) to start K absorption. After 4 h, the roots were washed with water and the plants were separated into roots, rosette leaves, bolts, cauline leaves, seedpods, foliar buds, and flowers. Each part was attached to a mount using an adhesive tape and covered with polyethylene film. The samples were analyzed using RRIS in the same way as the test for range determination and the radioactivities were measured using a gamma counter (ARC-300, ALOKA).

3. Results and discussion

3・1 Lower and upper limit of quantification

To confirm the validity of radiation from ^{42}K with existing detection methods, spots of standard solution were measured using RRIS. A lower limit of quantitation by RRIS was defined as $3 \times \sigma$ (σ = standard deviation of background intensities). The averages (and standard devia-

Table 1 The properties of ^{42}K detection by RRIS. The lower limit was calculated as three-fold standard deviations of the background intensity. The dynamic range is a ratio between the upper and lower limits.

	3 m	5 m	10 m	15 m
RRIS				
The lower limit (Bq/mm^2)	1.0×10^{-1}	9.1×10^{-2}	5.6×10^{-2}	2.2×10^{-2}
The upper limit (Bq/mm^2)	4.8×10^{2}	4.8×10^{2}	2.4×10^{2}	2.4×10^{2}
The dynamic range	4.7×10^{3}	5.2×10^{3}	4.3×10^{3}	1.1×10^{4}
The coefficient of determination R^2	0.9921	0.9908	0.9928	0.9923

tions) of background intensities of 3, 5, 10, 15-m detection were 1.5 (1.2), 1.7 (1.8), 3.3 (2.5) and 3.2 (2.5) counts/mm^2 respectively. The calculated lower limits of quantitation by RRIS for several detection times (3 – 15 m) varied from 2.2×10^{-2} Bq/mm^2 (15 m) to 1.0×10^{-1} Bq/mm^2 (3 m) as shown in Table 1, indicating that longer detection time resulted in a better lower limit.

To determine the upper limit of quantification, signal intensities of the standard spots were plotted, and these had radioactivities that were higher than the lower limit (Fig. 2 a). The signal intensity was obtained from region-of-interest (ROI) which was the same area where the drop of a standard spot was spread. Furthermore, calibration curves were drawn from the lowest to the highest point to provide coefficients of determination, where $R^2 > 0.99$. Here the highest point was defined as the upper limit. When the ROI was set as an actual spot size, the upper limits of quantification were shown to be either 250 Bq/mm^2 (10 and 15 m) or 500 Bq/mm^2 (3 and 5 m) (Fig. 2 b). The upper limits for each detection time were in the order of 10^2 and the dynamic ranges (a ratio between the highest and lowest points in the calibration plots) were approximately 5.0×10^3 independent of detection times, except for detection at 15 m, 1.1×10^4 (Table 1). These resulted from the RRIS property that the number of photons countable by RRIS per unit of time was definite[19]. In RRIS, only one photon can be detected per one pixel per one frame. Accordingly, the upper limits became much higher (> 500 Bq/mm^2) when the size of ROIs were increased by 4 to 25 times (Fig. 2 c), as a consequence of a decreased proportion of saturated pixels in ROIs. Setting ROIs larger has an advantage to pick up the diffused radiations and this is helpful especially for strong radiation emitter as ^{42}K whose radiations go through the plant tissues to diffuse easily.

3·2 Self-absorption by plant tissue

To assess the practical use of ^{42}K for plant physiology research, the quantitative efficiency of radiation from various tissues of *Arabidopsis* was investigated. Signal intensities from roots, rosette leaves, bolts, cauline leaves, seedpods, foliar buds, and flowers detected by RRIS were plotted against the number of counts detected by the gamma counter, which were considered to be proportional to the actual radioactivities in the tissues (Fig. 3). The transport of ^{42}K to flowers or seedpods was in such low quantities that detectable signals could not be secured. In the case that a measurable amount of energy emitted from ^{42}K contained within the plant tissue is absorbed by the plant tissue itself, the efficiency of detection of ^{42}K should be low, and thus the slope of the calibration curve should be remarkably decreased. This phenomenon of

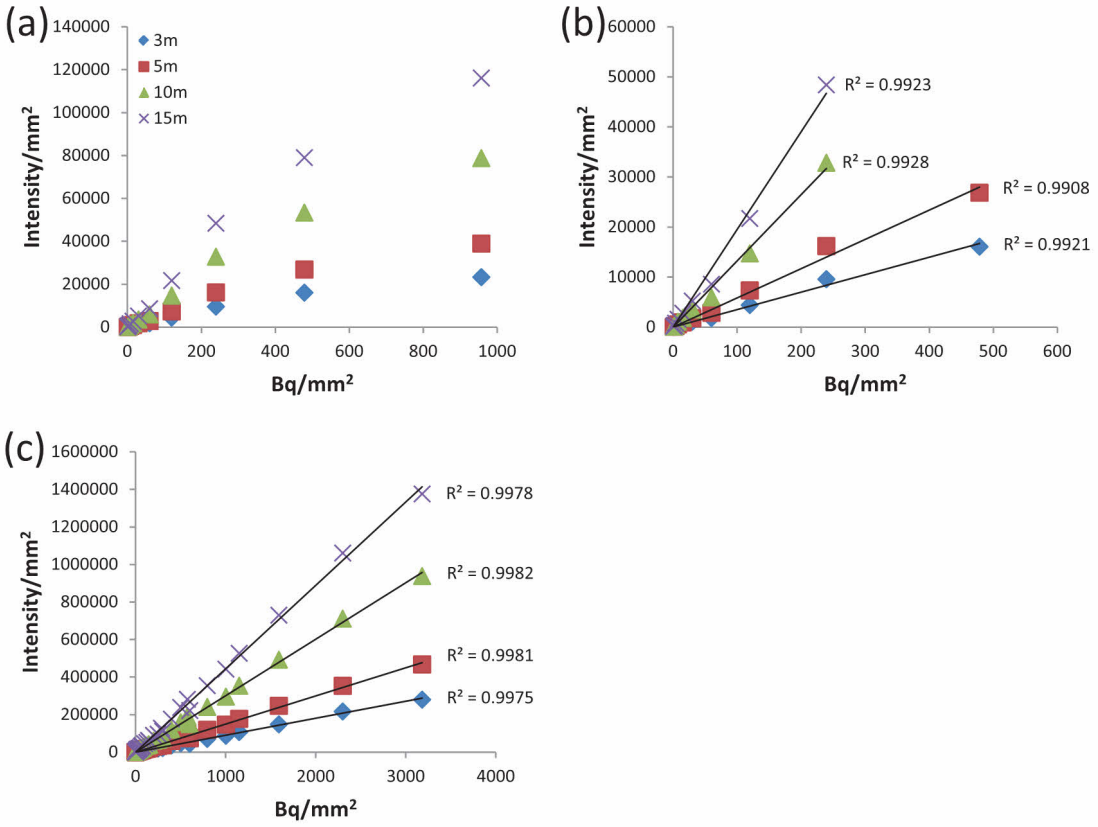

Fig. 2 (a) Signal intensity (Intensity/mm^2) detected by RRIS (real-time radioisotope imaging system) is plotted against radioactivity (Bq/mm^2) measured by liquid scintillation counter when ROIs were set as spot sizes. The background value was subtracted from each measured value. (b) Calibration curves drawn between the lowest point and the highest point show R^2 values larger than 0.99. (c) Signal intensities and calibration curves when ROIs were expanded to cover entire signals.

self-absorption has been observed in the detection of low-energy radiation from thick tissues[19]. The signals detected by RRIS and the counts detected by the gamma counter of whole tissues were well correlated with R^2 values of approximately ≥ 0.9 (Fig. 3 a), and the slopes of the individual calibration curves for these tissues, except for roots, were approximately 20 (19.1 − 22.6) within range of approximately 15% difference (Table 2). Based on a lack of significant difference between the slopes in plots of data for the thick bolt tissue and the thin leaf tissue, we suggest that the ^{42}K radiation is scarcely affected by self-absorption. In the case of the root, the slope of the calibration curve (29.4) was higher than the other tissues (Fig. 3, Table 2). It is possible that self-absorption was extremely small in the root, but the result remains to be elucidated, particularly because the sample volume of the root was small (n = 4) (Fig. 3 f). For the practical application of RRIS, a correction based on the calibration curve for each tissue would enable precise quantification of sequential images.

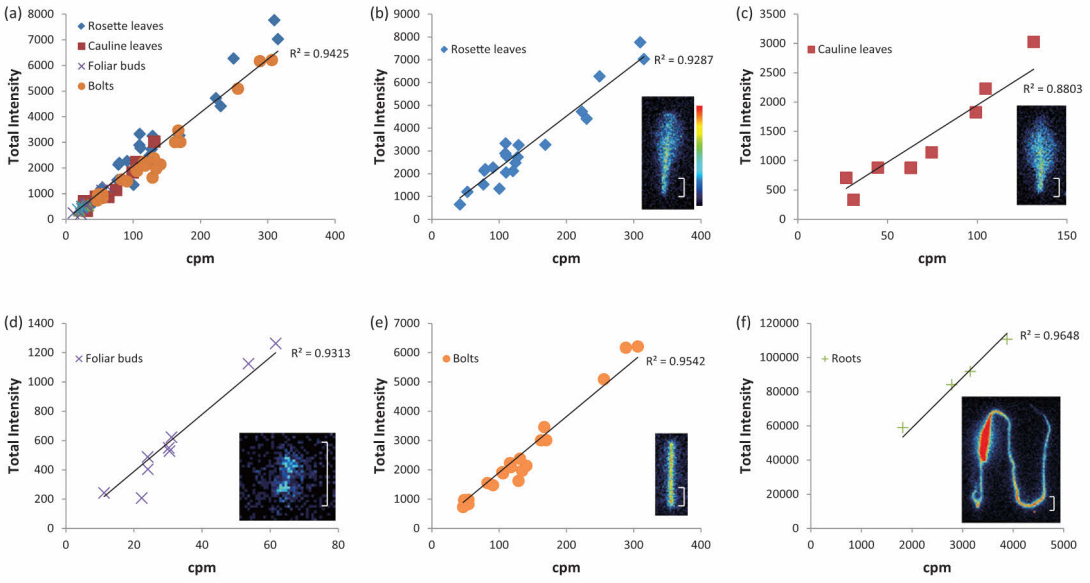

Fig. 3 (a) Signal intensities detected by RRIS (real-time radioisotope imaging system) plotted against the counts detected by the gamma counter for various plant tissues. Calibration curves were drawn from plots of tissues (rosette leaves, cauline leaves, foliar buds, bolts). (b) rosette leaves, (c) cauline leaves, (d) foliar buds, (e) bolts, and (f) roots. The representative example of an RRIS image on each tissue was shown on the right bottom of the plot. All scale bars represented 1 cm and the color bar in (b) was common among (b) to (f).

Table 2 Calibration curve parameters of various tissues analyzed by RRIS (real-time radioisotope imaging system). The slopes were calculated from the calibration curve of each tissue in Fig. 3.

	Calibration curve slope	Coefficient of determination (R^2)	number of measured sample
Rosette leaves	22.6	0.9287	21
Cauline leaves	19.5	0.8803	9
Foliar buds	19.5	0.9313	9
Bolts	19.1	0.9542	20
Roots	29.4	0.9648	4

3・3 Possibility of using the ^{42}K tracer experiment for an intact plant

One inherent feature of the ^{42}Ar–^{42}K generator is that the maximum amount of ^{42}K that can be produced at a time is only 10 kBq. Furthermore, the half-life of ^{42}K is 12 h, which means that the total radioactivity is remarkably decayed after several hours of imaging. On the other hand, the high-energy β-rays emitted from ^{42}K were shown to operate in favor of RRIS imaging. Detection of radiation by RRIS depends on the dose of radioactivity, which is determined by how efficiently the radiation is converted to signal intensity. In addition, the larger signal intensity makes counting errors smaller, and provides a good signal-to-noise ratio that enables high-precision analysis. The conversion efficiency of ^{42}K by RRIS was calculated as the ratio of intensity to radioactivity (Bq) by least-squares method, which was 444.75 when the detection time was 15 m, and is apparent in the slope of the calibration curve

in Fig. 2. Other radionuclides ^{22}Na, ^{65}Zn, ^{86}Rb, ^{109}Cd, ^{137}Cs, and ^{28}Mg have been previously tested, and the ratios of intensity to radioactivity (Bq) were 330.55, 13.371, 412.79, 77.981, 305.61, and 692.3 respectively[19),23)]. Compared with these radionuclides, the radiation from ^{42}K efficiently contributed to the signal intensity, thus, the high-energy β-rays easily reached the scintillator for conversion into photons. In addition, it is advantageous for imaging experiments that self-absorption hardly contribute to reducing the ^{42}K radiation. This study demonstrates that the generator-derived ^{42}K can be used for quantitative imaging experiments analyzed by RRIS, and could be a useful tool for plant physiology research.

Acknowledgement

We thank the ^{42}Ar–^{42}K generators for Japan Radioisotope Association. This work was supported by a grant from the Ministry of Agriculture, Forestry, and Fisheries of Japan (Genomics-based Technology for Agricultural Improvement, LCT-0002).

References

1) Schachtman, D. P., Schroeder, J. I., Lucas, W. J., Anderson, J. A. and Gaber, R. F., Expression of an inward-rectifying potassium channel by the *Arabidopsis KAT1* cDNA, *Science*, **258**, 1654-1658 (1992)
2) Schachtman, D. P. and Schroeder, J. I., Structure and transport mechanism of a high-affinity potassium uptake transporter from higher plants, *Nature*, **370**, 655-658 (1994)
3) Véry, A.-A., Nieves-Cordones, M., Daly, M., Khan, I., Fizames, C. and Sentenac, H., Molecular biology of K^+ transport across the plant cell membrane : What do we learn from comparison between plant species?, *J. Plant Physiol.*, **171**, 748-769 (2014)
4) Jeschke, W. D. and Pate, J. S., Cation and chloride partitioning through xylem and phloem within the whole plant of *Ricinus Communis* L. under conditions of salt stress, *J. Exp. Bot.*, **42**, 1105-1116 (1991)
5) Hayashi, H. and Chino, M., Collection of pure phloem sap from wheat and its chemical composition, *Plant Cell Physiol.*, **27**, 1387-1393 (1986)
6) Gaymard, F., Pilot, G., Lacombe, B., Bouchez, D., Bruneau, D., Boucherez, J., Michaux-Ferrière, N., Thibaud, J. B. and Sentenac, H., Identification and disruption of a plant shaker-like outward channel involved in K^+ release into the xylem sap, *Cell*, **94**, 647-655 (1998)
7) Glass, A., The regulation of potassium absorption in barley roots, *Plant Physiol.*, **56**, 377-380 (1975)
8) Gierth, M., Mäser, P. and Schroeder, J. I., The potassium transporter *AtHAK5* functions in K^+ deprivation-induced high-affinity K^+ uptake and *AKT1* K^+ channel contribution to K^+ uptake kinetics in Arabidopsis roots, *Plant Physiol.*, **137**, 1105-1114 (2005)
9) Läuchli, A. and Epstein, E., Transport of potassium and rubidium in plant roots : The significance of calcium, *Plant Physiol.*, **45**, 639-641 (1970)
10) Marschner, H. and Schimansky, C., Suitability of using rubidium-86 as a tracer for potassium in studying potassium uptake by barley plants, *J. Plant Nutr. Soil Sci.*, **128**, 129-143 (1971)
11) Takami, A., Yoshida, K., Tadokoro, H., Kitsukawa, S., Shimada, K., Sato, M., Suzuki, K., Masuda, Y. and Tanada, S., Uptakes and images of ^{38}K in rabbit heart, kidney, and brain, *J. Nucl. Med.*, **41**, 763 (2000)
12) Tanoi, K., Hojo, J., Suzuki, K., Hayashi, Y., Nishiyama, H. and Nakanishi, T. M., Analysis of potassium uptake by rice roots treated with aluminum using a positron emitting nuclide, ^{38}K, *Soil Sci. Plant Nutr.*, **51**, 715-717 (2005)
13) Nagatsu, K., A novel way of producing an aqueous solution of $^{38}K^+$ via the ^{40}Ar (p, 3n)-process, *Appl. Radiat. Isotopes*, **49**, 1505-1510 (1998)
14) Coskun, D., Britto, D. T. and Kronzucker, H. J., Regulation and mechanism of potassium release from barley roots : An *in planta* $^{42}K^+$ analysis, *New Phytol.*, **188**, 1028-1038 (2010)

15) Schulze, L. M., Britto, D. T., Li, M. and Kronzucker, H. J., A pharmacological analysis of high-affinity sodium transport in barley (*Hordeum Vulgare* L.): A $^{24}Na^{+}/^{42}K^{+}$ study, *J. Exp. Bot.*, **63**, 2479-2489 (2012)

16) Jahnke, S., Menzel, M. I., van Dusschoten, D., Roeb, G. W., Bühler, J., Minwuyelet, S., Blümler, P., Temperton, V. M., Hombach, T., Streun, M., Beer, S., Khodaverdi, M., Ziemons, K., Coenen, H. H. and Schurr, U., Combined MRI-PET dissects dynamic changes in plant structures and functions, *Plant J.*, **59**, 634-644 (2009)

17) Kawachi, N., Sakamoto, K., Ishii, S., Fujimaki, S., Suzui, N., Ishioka, N. S. and Matsuhashi, S., Kinetic analysis of carbon-11-labeled carbon dioxide for studying photosynthesis in a leaf using positron emitting tracer imaging system, *IEEE T. Nucl. Sci.*, **53**, 2991-2997 (2006)

18) Kanno, S., Yamawaki, M., Ishibashi, H., Kobayashi, N. I., Hirose, A., Tanoi, K., Nussaume, L. and Nakanishi, T. M., Development of real-time radioisotope imaging systems for plant nutrient uptake studies, *Philos. T. Roy. Soc. B*, **367**, 1501-1508 (2012)

19) Sugita, R., Kobayashi, N. I., Hirose, A., Tanoi, K. and Nakanishi, T. M., Evaluation of *in vivo* detection properties of ^{22}Na, ^{65}Zn, ^{86}Rb, ^{109}Cd and ^{137}Cs in plant tissues using real-time radioisotope imaging system, *Phys. Med. Biol.*, **59**, 837-851 (2014)

20) Fujiwara, T., Hirai, M. Y., Chino, M., Komeda, Y. and Naito, S., Effects of sulfur nutrition on expression of the soybean seed storage protein genes in transgenic petunia, *Plant Physiol.*, **99**, 263-268 (1992)

21) Homareda, H. and Matsui, H., Biochemical utilization of ^{42}Ar—^{42}K generator—Measurement of specific K^{+} binding to Na^{+}, K^{+}-ATPase—, *RADIOISOTOPES*, **35**, 543-546 (1986)

22) Wegmann, H., Huenges, E., Muthig, H. and Morinaga, H., Acceleration of tritons with a compact cyclotron, *Nucl. Instrum. Methods*, **179**, 217-222 (1981)

23) Sugita, R., Kobayashi, N. I., Saito, T., Hirose, A., Iwata, R., Tanoi, K. and Nakanishi, T. M., Quantitative analysis of ^{28}Mg in *Arabidopsis* using real-time radioisotope imaging system (RRIS), *RADIOISOTOPES*, **63**, 227-237 (2014)